

# Piezoelectric coefficients by molecular dynamics simulations in the constant stress ensemble: A case study of quartz

Daniel Herzbach<sup>a</sup> Martin H. Müser<sup>b,2,\*</sup>

<sup>a</sup>*Institut für Physik, WA 331, Universität Mainz, 55099 Mainz, Germany*

<sup>b</sup>*Department of Applied Mathematics, U.W.O., London, Ontario N6A 5B7, Canada*

---

## Abstract

Piezoelectric (strain) coefficients  $d_{ij}$  of quartz are calculated in terms of molecular dynamics as a function of pressure and temperature. We review the necessary formulas for the computation of electromechanical materials coefficients obtained at constant stress and temperature, and discuss how to overcome complications of the definition of polarization variations due to fluctuating box geometries. A method is employed suppressing significantly stochastic fluctuations of the estimators for piezoelectric coefficients. A recently suggested force field for the simulation of SiO<sub>2</sub> reproduces available experimental data quite accurately. Predictions are made for the pressure dependence of  $d_{ij}$  of quartz.

*Key words:* molecular dynamics simulations, piezoelectricity, quartz

*PACS:* 77.65.-j, 02.70.Ns, 62.20.Dc

---

## 1. Introduction

Dielectric properties of materials play an important role in many technological applications. It is therefore desirable to have methods at hand that allow one to compute dielectric, piezoelectric and related tensors in atomistic simulations. Dielectric properties are more challenging to calculate than thermal and mechanical properties, because the definition of polarization in periodically repeated cells is less obvious than the for-

mulation of thermo-mechanical variables. The reason is that an electrical dipole, and hence the polarization, lives on the surface of a sample. One of the consequences for computer simulations is that the value of the dipole depends upon where we chose the ‘central image’ of the periodically repeated cell to be. Conversely, internal energy, lattice parameters, strain, etc., are independent of the central image’s position. As we will outline further below, the ambiguity in defining the polarization becomes particularly delicate, even in classical molecular dynamics simulations, when one treats a system containing free charges at finite temperature and constant stress, which implies fluctuating box shapes.

Despite the mentioned ambiguity in the definition of polarization in periodic cells, it has been shown that there is a bulk or proper polarization that is intrinsic

---

\* Corresponding Author:

*Email address:* mmuser@uwo.ca (Martin H. Müser).

<sup>1</sup> DH gratefully acknowledges support from the BMBF through Grant 03N6015 and from the Materialwissenschaftliche Forschungszentrum Rheinland-Pfalz as well as stimulating discussions with Dr. U. Fotheringham and Dr. M. Letz (SCHOTT Glas).

<sup>2</sup> MHM gratefully acknowledges support from SharcNet (Ontario, Canada) and NSERC (Canada).

to the crystal and that is independent of the surfaces or the choice of the central image [1]. This proper polarization is obtained as the infinite wavelength limit of an appropriately defined Fourier transform of the dipole divided by the volume of the cell. The problem of defining the proper polarization for periodically repeated cells arises in force-field and *ab-initio* calculations. While a lot of work has been published on the calculation of the proper polarization in *ab-initio* calculations [2–5] much less attention has been paid to thermo-mechanical and dielectric properties obtained from calculations that are based on force fields. While such methods have been sketched in the literature, often in terms of harmonic approximations neglecting anharmonic fluctuation corrections [6], we are unaware of literature, in which (various) ways are stated explicitly how to calculate dielectric and piezoelectric susceptibility tensor in molecular dynamics or Monte Carlo simulations. We intend to fill this gap with a special focus on techniques related to Parrinello-Rahman type methods [7–11], which are used to maintain constant stress in atomistic simulations. The suggested ways to calculate electromechanical properties promise to be beneficial for the future, if *reliable*, transferable potentials become available so that complex structures can be studied that are not amenable to *ab-initio* simulations. This does not necessarily mean that the chemical composition of the unit cell of the material must be complex. Whenever quasi-harmonic approximations of high-temperature phases behave pathologically, as is the case for example in  $\beta$ -quartz, many independent configurations need to be produced in order to obtain meaningful averages for thermo-mechanical and dielectric properties. This is of course a very difficult task for *ab-initio* simulations. First-principle simulations can also be challenging when the unit cell becomes large. For example, using a simple model potential for  $\text{SiO}_2$ , it was found that quartz may undergo a phase transformation to a post quartz phase when shock compressed to a 50 GPa pressure, in which the new unit cell had a periodicity of 25 Å [12]. Such large length scales are currently not amenable to first-principle calculations.

In order to provide expressions for the calculation of electromechanical coefficients at finite temperatures, we discuss the free energy of a dielectric as a function of bulk polarization and strain as well as of the geometry of the periodically repeated (simulation) cell.

From this we will derive estimators for the calculation of the piezoelectric coefficients. One method will be based on relating response functions to fluctuations of observables, the other method will be based by explicitly applying an external electrical field. In the latter case, we show that stochastic errors in the coefficients can become extremely small despite strong thermal fluctuations if two simulations are run in parallel. In one simulation, the field is slowly increased as a function of time and the response  $R_1$  of the system is recorded. The other simulation is started with the same initial configuration and is thermostated with exactly the same random numbers. The response  $R_2$  observed in this run is subtracted from  $R_1$  to yield an output that is almost free of noise.

A similar stochastic difference method had been suggested by Ciccotti and Jacucci, [13] who were interested in the dynamics of a charged Lennard-Jones particle immersed in a fluid and subjected to an external field. It has been shown that the subtraction of two random signals, in which one system is propagated with external field and the other without external field, will have a large standard deviation if the system has large Lyapunov exponents. [14] This means that one should expect good signal-to-noise ratios for a crystalline material when using the above-described stochastic difference method.

The presented methodology will then be applied to quartz at various temperatures and pressures. Recent experiments indicate a loss of desired piezoelectric activity of  $\alpha$  quartz that occurs upon heating already 250 K below the  $\alpha - \beta$  quartz phase transition temperature  $T_1$  [15]. Computer simulations may help to shed some light on the question what the reason for this loss is. We may note that the elastic constant  $C_{14}$ , which also requires the absence of inversion symmetry just like piezoelectricity, does not show any anomalies outside of the immediate vicinity of the  $\alpha - \beta$  phase transition, i.e.,  $C_{14}$  is essentially constant at temperatures  $T < T_1 - 50$  K, and  $C_{14}$  vanishes for symmetry reasons above  $T_1$ . Two different model potentials were used in this study, namely one potential parametrized by van Beest, Kramer, and van Santen (BKS) [16] one recently suggested force field by Tangney and Scandolo [17]

The remainder of this paper is organized as follows. We will discuss the methodology in the following section. In section 3, we will present the bulk of our re-

sults and we will conclude in section 4.

## 2. Theory and Methods

### 2.1. Notation

In the following, a vector  $\underline{v}$  denotes a column of numbers, while a transposed vector  $\underline{v}^t$  represents a row of numbers. The scalar product of two vectors  $\underline{u}^t$  and  $\underline{v}$  will be written as  $\underline{u}^t \underline{v}$ , while the result of the operation  $\underline{u} \underline{v}^t$  corresponds to a matrix of rank two (indicated by two lines under the letter representing the matrix). A gradient of the form  $\partial/\partial \underline{u}$  applied to a scalar function results in a transposed vector. Similar comments apply to pseudo vectors such as the strain in Voigt notation. In some cases, we will state indices explicitly and apply the Einstein summation convention. Note that all matrices below are square matrices except for those related to piezoelectric coefficients.

The geometry of a periodically repeated (simulation) cell will be defined by a symmetric matrix  $\underline{\underline{h}} = (\underline{a}, \underline{b}, \underline{c})$ , where the three vectors  $\underline{a}, \underline{b}, \underline{c}$  span a periodically repeated parallelepiped. In numerical treatments, one conveniently uses scaled coordinates  $\underline{s}_i$  to denote the position of atom  $i$  within the central image. Hence, each time an atom crosses a boundary, we add or subtract unity to the appropriate component  $s_{i,\alpha}$  in order to maintain the minimum image convention. Another scaled coordinate will be denoted by  $\underline{r}$ , which is identical to  $\underline{s}$  except that the integer manipulations are suppressed that ensure the minimum image convention. Thus, the ‘real’ position  $\underline{R}_i$  of a particle is given by the equation

$$\underline{R}_i = \underline{\underline{h}} \underline{r}_i. \quad (1)$$

The coordinates  $\underline{r}$  will be used to define reduced dipoles  $\underline{\underline{\mu}}_{\text{red}}$

$$\underline{\underline{\mu}}_{\text{red}} = \sum_i Q_i \underline{r}_i + \underline{\underline{h}}^{-1} \underline{\underline{\mu}}_i, \quad (2)$$

$Q_i$  being the charge associated with particle  $i$ , and  $\underline{\underline{\mu}}_i$  being an electric dipole that potentially lives on atom  $i$ , for instance if polarizable sites are employed.

### 2.2. Linear response

Starting point of our study is the isothermal (configurational) partition function  $Z_{h,D}(N, \beta)$  at fixed dielectric displacement  $\underline{D}$  and constant box geometry as defined by a symmetric matrix  $\underline{\underline{h}}$ . According to the regular rules of statistical mechanics,  $Z_{h,D}(N, \beta)$  reads

$$Z_{h,D}(N, \beta) = \int d\Gamma \delta(\underline{\underline{h}}(\Gamma) - \underline{\underline{h}}) \times \delta(\underline{D}(\Gamma) - \underline{D}) \exp\{-\beta\Phi(\Gamma)\}. \quad (3)$$

Here  $\int d\Gamma$  symbolizes an integral over the phase space, the  $\delta(\bullet)$ ’s are the delta functions singling out proper geometry and dielectric displacement, and  $\Phi(\Gamma)$  is the potential energy of the system as a function of phase space, i.e., as a function of  $\underline{\underline{h}}$  and the set of reduced coordinates  $\{\underline{s}\}$ . As usual, it is possible to define a free energy  $\mathcal{F}$  from the partition function via the equation

$$\mathcal{F}_{h,D}(N, \beta) = -k_B T \ln Z_{h,D}(N, \beta). \quad (4)$$

As outlined in more detail below, Eq. (4), together with the definition of  $Z_{h,D}(N, \beta)$  in Eq. (3), allows one to connect ensemble averages over phase space (as carried out in atomistic simulations) with phenomenological materials parameters. Here, we restrict ourselves to static properties of strain and polarization, however, similar statements hold as well for more general quantities including dynamic response functions [18–21].

In the theory of elasticity, it is common to express partition function and hence free energy  $\mathcal{F} = -k_B T \ln Z(N, \beta)$  as a function of the strain rather than of the matrix defining a periodically repeated parallelepiped. Unlike the box geometry, the definition of the strain does require a reference state or a reference geometry  $\underline{\underline{h}}_0$  of the system, which is typically chosen to reflect the thermal expectation value of  $\underline{\underline{h}}$  at a given temperature and externally imposed stress. The (Lagrangian) strain with respect to  $\underline{\underline{h}}_0$  can be written as [8]:

$$u_{\alpha\beta} = \frac{1}{2} \left\{ \left( \underline{\underline{h}}_0^{-1} \right)_{\alpha\gamma} h_{\gamma\delta} h_{\delta\epsilon} \left( \underline{\underline{h}}_0^{-1} \right)_{\epsilon\beta} - \delta_{\alpha\beta} \right\}, \quad (5)$$

where we used tensor notation instead of Voigt notation. In Eq. (5),  $\delta_{\alpha\beta}$  denotes the Kronecker symbol. Since the relation between  $\underline{\underline{h}}$  and  $\underline{u}$  is well defined for a given reference  $\underline{\underline{h}}_0$ , it is possible to calculate the free

energy as a function of  $\underline{\tilde{u}}$  in terms of a Taylor series expansion in  $\underline{\tilde{u}}$  away from a phase transition point, i.e.,

$$\mathcal{F}_{u,D} = \mathcal{F}_{h_0,D} + \frac{\partial \mathcal{F}_{h,D}}{\partial \underline{\tilde{h}}} \frac{\partial \underline{\tilde{h}}}{\partial \underline{\tilde{u}}} \Big|_{\underline{\tilde{h}_0}} \underline{\tilde{u}} + \dots \quad (6)$$

The new free energy depends on both, strains  $\underline{u}$  and dielectric displacement  $\underline{D}$ . In the following, we will group these variables together into a generalized strain  $\underline{\tilde{u}} = (u_1, \dots, u_6, D_1, \dots, D_3)^t$ , with  $(u_1, \dots, u_6)$  being the strain tensor in Voigt notation.

The generalized stresses  $\underline{\tilde{\sigma}}$  that are the conjugate thermodynamic variables to  $\underline{\tilde{u}}$  can be calculated as  $\underline{\tilde{\sigma}} = (1/V) \partial \mathcal{F}(N, \beta) / \partial \underline{\tilde{u}}$ . Away from a phase transition, it is possible to expand  $\mathcal{F}_{\underline{\tilde{u}}}$  into a power series around a reference strain  $\underline{\tilde{u}}_0$  (which one can usually set to zero if  $\underline{\tilde{u}}_0$  at the reference geometry), thus

$$V_0 \underline{\tilde{\sigma}} = \frac{\partial \mathcal{F}_{h,D}(N, \beta)}{\partial \underline{\tilde{u}}} + \frac{\partial^2 \mathcal{F}_{h,D}(N, \beta)}{\partial \underline{\tilde{u}}^t \partial \underline{\tilde{u}}} \delta \underline{\tilde{u}} + \dots, \quad (7)$$

where the derivatives are evaluated at  $\underline{\tilde{u}}_0$ , the relative generalized strain is  $\delta \underline{\tilde{u}} = \underline{\tilde{u}} - \underline{\tilde{u}}_0$ , and  $V_0$  denotes the volume of the system at the reference geometry. The (expectation value of the) generalized stress at  $\delta \underline{\tilde{u}} = 0$  will be called  $\underline{\tilde{\sigma}}_0$  and  $\delta \underline{\tilde{\sigma}} = \underline{\tilde{\sigma}} - \underline{\tilde{\sigma}}_0$  denotes an (average) stress variation. One can then interpret the second-order derivative of  $\mathcal{F}_{\underline{\tilde{u}}}$  with respect to  $\underline{\tilde{u}}$  as generalized elastic constants  $\underline{\tilde{C}}$ , that connect  $\underline{\tilde{u}}$  and  $\underline{\tilde{\sigma}}$  via  $\underline{\tilde{\sigma}} = \underline{\tilde{C}} \underline{\tilde{u}}$ , or if we represent  $\underline{\tilde{u}}$  and  $\underline{\tilde{\sigma}}$  explicitly

$$\begin{pmatrix} \underline{u} \\ \underline{D} \end{pmatrix} = \begin{bmatrix} \underline{\underline{C}}_E^{-1} & \underline{\underline{d}}^t \\ \underline{\underline{d}} & \epsilon_0 \underline{\underline{\epsilon}}_{r,\sigma} \end{bmatrix} \begin{pmatrix} \underline{\sigma} \\ \underline{E} \end{pmatrix}. \quad (8)$$

Here,  $\underline{\underline{C}}_E$  denotes ‘real’ elastic constants at constant (external) electric field and  $\underline{\underline{d}}$  are the piezoelectric strain coefficients.  $\underline{\underline{\epsilon}}_{r,\sigma}$  is the (isothermal) dielectric tensor at constant stress. Eq. (8) is a linear equation that connects  $\underline{\tilde{u}}$  with  $\underline{\tilde{\sigma}}$ .

Within linear-response theory,  $\underline{\tilde{u}}$  and  $\underline{\tilde{\sigma}}$  are conjugate to each other. In the constant- $\underline{\tilde{u}}$  ensemble, we can therefore attribute an excess free energy  $\Delta \mathcal{F}$  due to the fluctuations in  $\underline{\tilde{u}}$ , which is given by

$$\Delta \mathcal{F} = \frac{V_0}{2} \delta \underline{\tilde{u}}^t \underline{\tilde{C}} \delta \underline{\tilde{u}}. \quad (9)$$

Thermal fluctuations of  $\underline{\tilde{u}}$  at fixed  $\underline{\tilde{\sigma}}$  will thus be related to  $\underline{\tilde{C}}$ , which for harmonic approximations, results in

$$\left\langle \begin{bmatrix} \delta \underline{u} \delta \underline{u}^t & \delta \underline{u} \delta \underline{D}^t \\ \delta \underline{D} \delta \underline{u}^t & \delta \underline{D} \delta \underline{D}^t \end{bmatrix} \right\rangle = \frac{k_B T}{V_0} \begin{bmatrix} \underline{\underline{C}}_E^{-1} & \underline{\underline{d}}^t \\ \underline{\underline{d}} & \epsilon_0 \underline{\underline{\epsilon}}_{r,\sigma} \end{bmatrix}. \quad (10)$$

In this section, we have measured the free energy density by dividing the actual value of  $\mathcal{F}$  by the volume  $V_0$  of the reference strain. This convention, which is typically used in the theory of elasticity, is also beneficial when evaluating Eq. (10): The fluctuation of the electric displacement can be rewritten as fluctuation of the polarization  $\underline{P}$ . Introducing the dielectric susceptibility,  $\underline{\underline{\chi}} = \underline{\underline{\epsilon}}_r - \underline{\underline{1}}$ , we can rewrite Eq. (10) as:

$$\left\langle \begin{bmatrix} \delta \underline{u} \delta \underline{u}^t & \delta \underline{u} \delta \underline{P}^t \\ \delta \underline{P} \delta \underline{u}^t & \delta \underline{P} \delta \underline{P}^t \end{bmatrix} \right\rangle = \frac{k_B T}{V_0} \begin{bmatrix} \underline{\underline{C}}_E^{-1} & \underline{\underline{d}}^t \\ \underline{\underline{d}} & \epsilon_0 \underline{\underline{\chi}}_\sigma \end{bmatrix}. \quad (11)$$

Relations like Eqs. (7) and (11) can be exploited in atomistic calculations to determine the susceptibilities of interest. However, it will first be necessary to state the proper estimators for the polarization fluctuation.

### 2.3. Ambiguity of the dipole and its fluctuation

It is helpful to consider Fig. 1, in order to understand the difficulties with the formulation of bulk polarization alluded to in the introduction. Part (a) of Fig. 1 shows that the definition of the dipole  $\mu$  attributed to the simulation cell (from which the polarization follows) depends upon where we chose the boundary of the central cell to be. By displacing the boundary, none of the interatomic distances is altered, yet the dipole changes its value. As long as the shape (here simply the length) of the cell is maintained, this ambiguity causes no complications for the response functions, because we only need to know polarization differences. A polarization change is independent of the choice for the boundary - provided we keep track of the ‘true’ positions of the atoms, i.e., when a charged particle moves across a boundary we do not subtract unity of the scaled coordinate for the calculation of the dipole. Thus evaluating fluctuations related to dipoles (from which the constant-strain dielectric and piezoelectric constants could be calculated), do not depend on the choice for the position of the central image.

When the cell fluctuates, even a polarization difference will depend upon where we chose the central image to be. This is illustrated in part (b) of Fig. 1, where

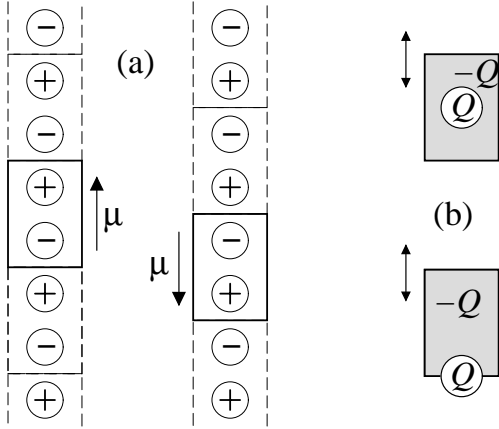


Fig. 1. Illustration of the ambiguity for (a) the definition of a dipole  $\underline{\mu}$  and for (b) the fluctuation of the dipole. The boxes framed by a solid line present the position of the central image, while boxes framed with a broken line are periodic images. The lower left corner of the central image is defined to the origin of the coordinate system. In part (b), a positive background neutralizes the point charge  $Q$  and the arrows with the two arrow heads represent fluctuation of the box geometry.

in one case, the reduced coordinates of a charged particle is constrained to zero (bottom) and in the other case it is set constant to one half (top). Both times, we assume the presence of an opposite background charge of constant density ensuring charge neutrality. In the upper part of Fig. 1 (b), the fluctuation of the dipole vanishes exactly if we keep the reduced positions of the charge  $Q$  fixed in the center of mass. Therefore, the fluctuation of the dipole will be zero in the upper half. In the bottom part, we would attribute a dipole to the cell, which would fluctuate with changing box size. Thus the dipole fluctuations is effected by the choice of the location for the central image.

The above mentioned difficulties do not arise if one deals with neutral molecules whose constituents have charges that add up to zero. In that case it is easy to remove the ambiguity due to surface effects or periodic-boundary conditions. One would only have to suppress any minimum image convention within the molecules, i.e., for the calculation of the dipole, the  $\underline{r}_i$  (see Sec. 2.1) have been to be defined such that two covalently bonded atoms are separated by the proper distance. In principle, it would be possible to define similar molecules in an ideal crystalline network such as quartz, i.e., by evaluating the dipole over

entities that consist of a central silicon atom and its four oxygen neighbors, where the charges of the O atoms would only count half, in order to avoid double counting. However, such ‘tricks’ cannot be generally applied, for instance, if any type of disorder or even impurities are present in the system, or if a non-rigid charge model is employed.

#### 2.4. Fluctuation estimators for dipoles

The problem of defining bulk dipoles can be overcome by considering the small wave length limit of the dipole’s spatial Fourier transform  $\tilde{\rho}(\underline{k})$ . If the box cell is fluctuating, it is appropriate to work with scaled reciprocal vectors  $\underline{k} = 2\pi(m_x, m_y, m_z)$  where the  $m_\alpha$  are integer numbers that are related to the true reciprocal vectors through  $\underline{K} = \underline{k} \underline{h}^{-1}$ . Since the box is fluctuating, it is more meaningful to work with reduced coordinates in both real and reciprocal space. Let us first consider the Fourier transform of the charge distribution  $\rho(\tilde{\underline{k}})$

$$\tilde{\rho}(\underline{k}) = \sum_i Q_i e^{i\underline{k} \cdot \underline{s}_i}. \quad (12)$$

It remains unchanged if we add or subtract unity from a particular  $\underline{s}_i$  or if we rescale the box geometry. Yet, if we formally differentiate  $\tilde{\rho}(\underline{k})$  with respect to  $\underline{k}$  (which one cannot do in practice as the  $k_\alpha$ ’s are discrete), then the derivative does not show the same invariance. The formal derivative of  $\tilde{\rho}(\underline{k})$  evaluated at  $\underline{k} = 0$  corresponds to the contribution of the reduced dipole due to the point charges, see Eq. (2).

If, however, one defines a reference configuration, which can be an initial configuration at time  $t = 0$  that does not have to be equilibrated, then the *difference* between a reduced dipole  $\underline{\mu}_{\text{red}}(t)$  evaluated at time  $t$  and the reference dipole  $\underline{\mu}_{\text{red}}(0)$  is invariant against the transformations discussed in Fig. 1 as long as we perform the transformation on the configuration of interest and the reference configuration. For the final evaluation of the dipole, we then multiply the value  $\underline{\mu}_{\text{red}}(0)$  with the expectation value of the box shape, thus, our estimator becomes

$$\underline{\mu}_{\text{est}} = \langle \underline{h} \rangle \underline{\mu}_{\text{red}} \quad (13)$$

and consequently that for the polarization  $\underline{P}_{\text{est}} = \underline{\mu}_{\text{est}} / \langle V \rangle$ . These estimators do not enable one to cal-

culate absolute dipoles or polarizations but only relative quantities, i.e., those to be used in Eq. (11) for the calculation of fluctuation relations. One possibility to obtain absolute values for the polarization could be to set up an initial configuration about which we know that its dipole vanishes, i.e., due to an underlying symmetry.

## 2.5. Direct estimators with noise reduction

Applying an external electrical field  $\underline{E}$  to the system is one possibility to evaluate piezoelectric coefficients and higher-order coefficients such as those related to electrostriction. The appropriate force that acts on the reduced coordinates related to a point charge  $Q_i$  would read  $\underline{h}^{-1} \underline{E} Q_i$ . It is yet not meaningful to simply add a term  $-\sum_i Q_i \underline{E}^t \underline{R}_i$  to the Hamiltonian. Such a perturbation would require to have a force act onto the shape of the simulation cell and this force would depend on whether a particle is counted within the central image or within a periodic image. We thus suppress the force from the external field onto the  $\underline{h}$  matrix, also because it would be absent in a system without charges and dipoles.

If the shape of the system is known for  $\underline{E} = 0$  and the initial configuration is equilibrated, then one may switch on the field adiabatically and monitor the box shape variation from which the strain can be calculated. This procedure will give correct results, in particular if one averages over an appropriate number of independent, initial configurations. However, this algorithm may produce large stochastic scatter in particular at elevated temperatures.

The noise can be reduced and the necessity of having to know the average structure can be omitted if one performs a reference simulation in which the electric field remains switched off. The reference simulation should be based on the same initial condition and an identical initialization of the thermostat. Any instantaneous configuration at finite field can be compared directly to the instantaneous configuration at zero field. Within a few molecular dynamics steps, it is then possible to obtain quite reasonable estimates for the piezoelectric and other dielectric coefficients, even if the system is rather anharmonic and contains slow modes, as is the case in quartz close to the  $\alpha - \beta$  transition. Fig. 2 confirms this expectation.

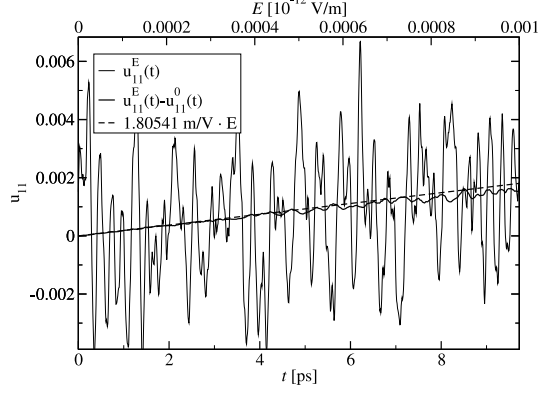


Fig. 2. Response of the strain  $u_{11}$  as a function of time (below) or electrical field (above) for an  $N = 1080$  particle system ( $\alpha$ -quartz) at temperature  $T = 300$  K. The long dashed line is the result for the piezoelectric coefficient based on evaluating the fluctuation relation in Eq. (11).

In Fig. 2, we increased the external field slowly with time and also chose box inertia sufficiently small to have the cell shape adapt quickly to the new field. We thermostated the box geometry with a Langevin thermostat to decrease the (stochastic) correlation time. Excellent estimates for the piezoelectric coefficients can be obtained already after one hundred MD steps by evaluating the slope  $\partial u_{11} / \partial E_x$ . In this way, four simulations have to be run to determine all generalized elastic constants discussed in this paper; three in which the electric field is parallel to one of the three coordinate axis and one in which the electric field remains zero. Again, we would like to stress that in all four runs the same initial conditions (one large sample in thermal equilibrium or an average over some small equilibrated samples) must be used as an input into the simulation and that all runs require the same random number sequence.

For the various silica polymorphs investigated here, we obtain a statistical accuracy of better than 5% for the  $d_{ij}$ 's if we first equilibrate the material for about 10,000 MD steps to produce an equilibrated start configuration. Note that it takes relatively long to equilibrate crystalline quartz above room temperature, although quartz is crystalline. This is because it has an unusually large phonon density of states at small frequencies. The start configuration is then used for four independent runs, namely one without electric field plus three runs with electric field in one of the three

spatial dimensions. Each of these runs is about 2,500 MD steps long and produces a graph similar to that shown in Fig. 2. Thus, the required numerical effort to obtain the data is relatively small.

Using Nosé Hoover thermostats or related (less sophisticated) rescaling methods do probably not lead to similarly reliable results. In particular for large systems and/or small temperatures, the motion of the simulation cell will be quite harmonic and thus the (crucial!) exchange of (kinetic) energy between the simulation cell and the internal degrees of freedom will be inefficient. This inefficiency will prevent the cell from quickly finding its new preferred shape or from fluctuating around it. Also Monte Carlo methods (which are not necessarily the appropriate method for constant-stress ensemble to begin with) might need many more moves than constant-stress MD simulations in which the cell is thermostated stochastically. However, a similar methodology could yet be implemented and would probably yield more quickly converging results than a brute-force evaluation of fluctuation relations.

### 3. Results

$\alpha$ -quartz is one of the most commonly employed piezoelectric materials and is therefore an interesting candidate to investigate. Moreover, due to its many other technological uses and due to its geological abundance, it remains one of the most intensively studied materials. Since it is desirable to model such an important substance on time scales longer than those amenable to ab-initio based simulations, many model potentials have been put forth in the recent past. The goal is to develop a reliable model potential that allows one to simulate chemically realistically silica and silica derivatives. None of the model potentials known to us were adjusted to fit the mechano-electrical behaviour. Calculating the corresponding response functions thus provides an independent test of the usefulness and reliability of the approaches.

This test is particularly challenging because it is susceptible to the effective charges chosen for the ions. It is well known that effective charges should ideally be designed as tensor charges, however, none of those potentials with the aim to be potentially transferable have included non-isotropy of the charges. Only

non-transferable potentials were put forth for silica, in which the parameters describing the electrostatic interactions depended on the specific sites that oxygen atoms occupied in an ideal quartz lattice.

In this paper, we will limit our attention to the comparison of two trustworthy (and potentially transferable) approaches, namely the well-established potential by van Beest, Kramer, and van Santen (BKS) which has been used very successfully in the last decade for both ordered and disordered silica, and a new potential suggested recently by Tangney and Scandolo (TS). Both are rigid-ion potentials, however, the TS potential is parametrized as a fluctuating dipole potential, i.e., the oxygen atoms are treated as being polarizable. The dipoles are obtained by minimizing a potential energy function (self-consistently) with respect to the dipoles. More details on the potentials can be found in the original literature and also in a future, more exhausting comparison of the performance of these two potentials and a fluctuating charge potential [22]. At this point, we only wish to comment that the TS potential performs extremely well in essentially all thermo-mechanical properties. In particular, it is the only one of the tested potentials that produces the  $c/a$  anomaly in the two independent lattice constants at the  $\alpha$ - $\beta$  transition of quartz as observed experimentally.

#### 3.1. Temperature dependence of $d_{11}$ in $\alpha$ quartz

The temperature dependence of piezoelectric constants is of technological relevance because one is often interested in having pressure sensors and pressure transducers at varying temperatures. One of the few disadvantages of  $\alpha$ -quartz is the relatively low transition temperature to  $\beta$ -quartz, in which  $d_{11}$  is symmetry-forbidden. This means that quartz cannot be used as an effective piezoelectric material at high temperature. In this subsection, we will first show that both BKS and TS can be used to reproduce available experimental data for the piezoelectric strain coefficients at least semi-quantitatively and then analyze the piezoelectric properties of the two hypothetical post quartz phases suggested recently [23].

Fig. 3 shows the temperature dependence of the piezoelectric strain strain coefficient  $d_{11}$ . One can see that both potentials underestimate the value of  $d_{11}$ ,

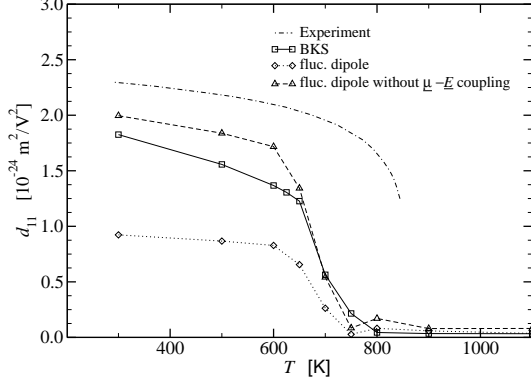


Fig. 3. Comparison of the temperature dependence of the piezoelectric strain coefficient  $d_{11}$  between experiment and simulation. The BKS (squares) and the TS potential were used. In the TS potential, two set of runs were performed, one in which the electric field was coupled to the dipoles (diamonds), and one in which this coupling was suppressed (triangles).

the TS potential underestimates its value in the low-temperature phase by more than 50%. The discrepancy between experiment and TS potential is surprising due to the otherwise good performance of the TS potential. We therefore speculated that Tangney and Scandolo parametrized quantum-chemical effects into the dipoles and re-ran the simulations without coupling the dipoles to the electric field, so that only the bare charges coupled to  $\underline{E}$ . Our speculation was supported by observing a large correlation between the magnitude of an individual dipole on an oxygen atom and the bending angle of the Si-O-Si bonds. By suppressing the coupling to the electric field (or by only including bare charges in the calculation of the polarization fluctuations), the discrepancy between the TS potential and experiment is significantly reduced and quantitative agreement is almost achieved, except for an  $\mathcal{O}(15)\%$  error in the transition temperature.

It may appear surprising that (short-range) quantum chemical effects can be absorbed into dipolar interactions. However, the four dipoles associated with the oxygen forming the vortices of a tetrahedral  $\text{SiO}_4$  unit typically add up to a value close to zero. Therefore the effects of the dipoles in the simulation is effectively short-range in nature as well.

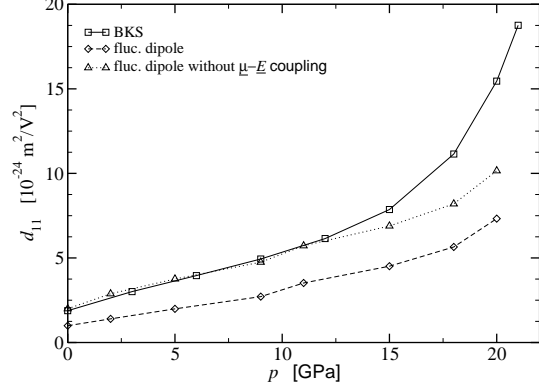


Fig. 4. Pressure dependence of the strain coefficients  $d_{11}$  in  $\alpha$ -quartz. The same symbols as in the previous figure were used.

### 3.2. Pressure dependence of $d_{11}$

The pressure dependence of quartz-like materials has remained of interest to current research, see for instance, Ref. [24], which is part of our motivation for our pressure study. In Fig. 4, we show the pressure dependence of the piezoelectric strain coefficient of quartz, which was calculated using the same approaches as in the Fig. 3. While we believe that the most accurate data is obtained with TS by suppressing the coupling between  $\underline{\mu}$  and  $\underline{E}$ , we include the other two approaches for comparison.

The TS potential without  $\underline{\mu}\text{-}\underline{E}$  coupling and the BKS potential show surprisingly strong similarity up to 12 GPa. Above this pressure, the results for the piezoelectric coefficients are starting to differ. Keeping in mind that the transition pressure for the  $\alpha \rightarrow II$  transition is smaller in BKS than in TS [22], it is obvious that the results differ dramatically on approach to the transition pressure. The increase in the piezoelectric activity originates in the softening of internal modes in  $\alpha$ -quartz, in which the oxygen atoms are displaced with respect to the oppositely charged silicon atoms.

It would be interesting to analyze the piezoelectric strain coefficients experimentally up to the pressure at which the transition into the so-called quartz II phase takes place, because this might settle the ongoing debate regarding the degree of softening of quartz under increasing pressure.

## 4. Conclusions

In this paper, we discussed various methods to compute the piezoelectric response within the framework of molecular dynamics simulations that are based on classical force fields and that employ effective charges as well as (inducible) dipoles. Similar approaches can be derived for higher-order response functions such as electrostrictive coefficients. The difficulty of calculating quantities involving the electric polarization as compared to observables related to purely thermo-mechanical quantities lied in the fact that the dipole or polarization of the simulation cell is ill defined, in particular when the box geometry is allowed to fluctuate. Once this complication is overcome, we discussed one ‘traditional’ method based on the fluctuation dissipation theory by relating the fluctuations of observables to their appropriate response functions. While we only used this method to analyze static susceptibilities, it is easily generalized to dynamical response functions as well.

We also discussed an alternative method that allows one to calculate the static mechanical/dielectric response with small stochastic scatter at small computational cost even when strong thermal fluctuations were present. We applied the methodology to various silica polymorphs with an emphasis on quartz and post quartz phases. Two different model potentials were used for this study, namely the well-established (and slightly flawed) potential by van Beest, Kramer, and van Santen (BKS), [16] and the recently suggested potential by Tangney and Scandolo (TS) [?] that is parametrized as a fluctuating dipole potential.

The TS potential, which reproduces thermo-mechanical behaviour of  $\text{SiO}_2$  with high accuracy [22], only achieved good agreement with available experimental data when the electrical field was not coupled directly to the induced dipoles. We therefore speculate that effects that are quantum-chemical in nature were effectively parametrized into the dipolar interactions. Accepting this interpretation, TS reproduces the available experimental data within about 10% accuracy while BKS is within 15% accuracy. Keeping in mind that Tangney and Scandolo did not fit their model potential to any available data, one may be confident that the prediction based on their model are quite accurate, at least as long as silicon

atoms remain four coordinated.

We also calculated the pressure-dependence of the piezoelectric strain coefficients in  $\alpha$  quartz. No experiments are known to us, but we believe that such experiments would shed light on the softening of quartz under increasing pressure.

## References

- [1] R. M. Martin, *Phys. Rev. B* 5 (1972) 1607.
- [2] R. D. King-Smith, D. Vanderbilt, *Phys. Rev. B* 47 (1993) 1651.
- [3] L. Bellaiche, D. Vanderbilt, *Phys. Rev. B* 61 (2000) 7877.
- [4] D. Vanderbilt, *J. Phys. Chem. Solids* 61 (2000) 147.
- [5] R. E. Cohen, *J. Phys. Chem. Solids* 61 (2000) 139.
- [6] M. Born, K. Huang, *Dynamical Theory of Crystal Lattices*, Clarendon Press, Oxford, 1954.
- [7] M. Parrinello, A. Rahman, *Phys. Rev. Lett.* 45 (1980) 1196.
- [8] M. Parrinello, A. Rahman, *J. Appl. Phys.* 52 (1981) 7182.
- [9] M. Parrinello, A. Rahman, *J. Chem. Phys.* 76 (1980) 2662.
- [10] C. Cleveland, *J. Chem. Phys.* 89 (1988) 4987.
- [11] R. M. Wentzcovitch, *Phys. Rev. B* 44 (1991) 2358.
- [12] C. Campana, M. H. Müser, *High Press. Res.* 24 (2004) 517.
- [13] G. Ciccotti, G. Jacucci, *Phys. Rev. Lett.* 35 (1975) 789.
- [14] G. P. Morriss, D. J. Evans, E. G. D. Cohen, H. van Beijeren, *Phys. Rev. Lett.* 62 (1989) 1579.
- [15] J. Haines, O. Cambon, D. A. Keen, M. G. Tucker, M. T. Dove, *Appl. Phys. Lett.* 81 (2002) 2968.
- [16] B. van Beest, G. Kramer, R. van Santen, *Phys. Rev. Lett.* 64 (1990) 1955.
- [17] P. Tangney, S. Scandolo, *J. Chem. Phys.* 116 (2002) 14.
- [18] M. P. Allen, D. J. Tildesley, *Computer simulation of liquids*, Clarendon Press, Oxford, 1987.
- [19] D. Frenkel, B. Smit., *Understanding molecular simulation : from algorithms to applications*, Academic Press, San Diego, 1996.
- [20] J. M. Thijssen, *Computational physics*, Cambridge University Press, New York, 1999.
- [21] D. P. Landau, K. Binder, *A guide to Monte Carlo simulations in statistical physics*, Cambridge University Press, New York, 2000.
- [22] D. Herzbach, K. Binder, M. H. Müser, *J. Chem. Phys.* Submitted.
- [23] C. Campana, M. H. Müser, J. S. Tse, D. Herzbach, P. Schöffel, *Phys. Rev. B* 70 (2004) 224101.
- [24] J. Haines, O. Cambon, D. Cachau-Herreillat, G. Fraysse, M. F.E., *Solid State Sci.* 6 (2004) 995.